Iteratively Decoded Variable Length Space-Time Coded Modulation

S. X. Ng and L. Hanzo

School of ECS, University of Southampton, SO17 1BJ, UK.
Tel: +44-23-8059 3125, Fax: +44-23-8059 4508
Email: {sxn,lh}@ecs.soton.ac.uk, http://www-mobile.ecs.soton.ac.uk

Abstract – **An Iteratively Decoded Variable Length Space Time Coded Modulation (VL-STCM-ID) scheme capable of simultaneously providing both coding and iteration gain as well as multiplexing and diversity gain is proposed. Non-binary unity-rate precoders are employed for assisting the iterative decoding of the VL-STCM-ID scheme. The discrete-valued source symbols are first encoded into variable-length codewords that are mapped to the spatial and temporal domains. Then the variable-length codewords are interleaved and fed to the precoded modulator. More explicitly, the proposed VL-STCM-ID arrangement is a jointly designed iteratively decoded scheme contriving source coding, channel coding, modulation and spatial diversity/multiplexing. As expected, the higher the source correlation, the higher the achievable performance gain of the scheme becomes. Furthermore, the performance of the VL-STCM-ID scheme is more than 14 dB better than that of the Fixed Length STCM (FL-STCM) benchmarker at a source symbol error ratio of** 10^{-4}**.**

1. INTRODUCTION

Shannon's separation theorem stated that source coding and channel coding is best carried out in isolation [1]. However, this theorem was formulated in the context of potentially infinite-delay, lossless entropy-coding and infinite block length channel coding. In practise, real-time wireless audio/video communications systems do not meet these ideal hypotheses. Explicitly, the source encoded symbols often remain correlated, despite the lossy source encoder's efforts to remove all redundancy. Furthermore, they exhibit unequal error sensitivity. In these circumstances, it is often more efficient to use jointly designed source and channel encoders.

The wireless communication systems of future generations are required to provide reliable transmissions at high data rates in order to offer a variety of multimedia services. Space time coding schemes, which employ multiple transmitters and receivers, are among the most efficient techniques designed for providing high data rates by exploiting the high channel capacity potential of Multiple-Input Multiple-Output (MIMO) channels [2, 3]. More explicitly, Bell-lab's LAyered Space Time architecture (BLAST) [4] was designed for providing full transmitter-multiplexing gain, while Space Time Trellis Codes (STTC) [5] were designed for providing full transmitter-diversity gain.

In this contribution, we describe a jointly designed source coding and Space Time Coded Modulation (STCM) scheme, where two dimensional (2D) Variable Length Codes (VLCs) are transmitted by exploiting both the spatial and temporal domains. More specifically, the number of activated transmit antennas equals the number of symbols of the corresponding VLC codeword in the spatial domain, where each VLC codeword is transmitted during a single symbol period. Hence, the transmission frame length is determined by the fixed number of source symbols and therefore the proposed Variable Length STCM (VL-STCM) scheme does not exhibit synchronisation problems and does not require the transmission of side information. Additionally, the associated source correlation is converted into an increased product distance, hence resulting in an increased coding gain. Furthermore, the VL-STCM scheme is capable of providing both multiplexing and diversity gains with the aid of multiple transmit antennas.

It was shown in [6] that a binary unity-rate precoder can be serially concatenated with Trellis Coded Modulation (TCM) [7] for the sake of invoking iterative detection and hence for attaining iteration gains. Since VL-STCM also belongs to the TCM family, we further develop the VL-STCM scheme for attaining additional iteration gains by introducing non-binary unity-rate precoders between the variable-length space-time encoder and the modulator. The Iteratively Decoded (ID) VL-STCM (VL-STCM-ID) scheme achieves a significant coding/iteration gain over both the non-iterative VL-STCM scheme and the Fixed Length STCM (FL-STCM) benchmarker.

The rest of the paper is organised as follows. The overview of the space-time coding technique advocated is given in Section 2 and the 2D VLC design is outlined in Section 3. The description of the proposed VL-STCM and VL-STCM-ID schemes is presented in Sections 4 and 5, respectively. In Section 6, the performance of the proposed schemes is discussed and finally our conclusions are offered in Section 7.

The financial support of the EPSRC, Swindon UK and the EU under the auspices of the PHOENIX and NEWCOM projects is gratefully acknowledged.

2. SPACE TIME CODING OVERVIEW

Let us consider a MIMO system employing N_t transmit antennas and N_r receive antennas. The signal to be transmitted from transmit antenna m, $1 \leq m \leq N_t$, at the discrete time index t is denoted as $x_m[t]$. The signal received at antenna n, $1 \leq n \leq N_r$, and at time instant t can be modelled as:

$$r_n[t] = \sqrt{E_s}\sum_{m=1}^{N_t} h_{n,m}[t]x_m[t] + w_n[t] , \quad (1)$$

where E_s is the average energy of the signal constellation, $h_{n,m}[t]$ denotes the flat-fading channel coefficients between transmit antenna m and receive antenna n at time instant t, while $w_n[t]$ is the Additive White Gaussian Noise (AWGN) having zero mean and a variance of $N_0/2$ per dimension. The amplitude of the modulation constellation points is scaled by a factor of $\sqrt{E_s}$, so that the average energy of the constellation points becomes unity and the expected Signal-to-Noise Ratio (SNR) per receive antenna is given by $\gamma = N_t E_s/N_0$ [8]. Let us denote the transmission frame length as T symbol periods and define the space-time encoded codeword as an $(N_t \times T)$-dimensional matrix $\mathbf{C}$ formed as:

$$\mathbf{C} = \begin{bmatrix} c_1[1] & c_1[2] & \ldots & c_1[T] \\ c_2[1] & c_2[2] & \ldots & c_2[T] \\ \vdots & \vdots & \ddots & \vdots \\ c_{N_t}[1] & c_{N_t}[2] & \ldots & c_{N_t}[T] \end{bmatrix} , \quad (2)$$

where the tth column $\mathbf{c}[\mathbf{t}] = [c_1[t]\ c_2[t] \ldots\ c_{N_t}[t]]^T$ is the space-time symbol transmitted at time instant t and the mth row $\mathbf{c_m} = [c_m[1]\ c_m[2] \ldots\ c_m[T]]$ is the space-time symbol transmitted from antenna m. The signal transmitted at time instant t from antenna m, which is denoted as $x_m[t]$ in Equation 1, is the modulated space-time symbol given by $x_m[t] = f(c_m[t])$ where $f(.)$ is the modulator's mapping function. The Pair-Wise Error Probability (PWEP) of erroneously detecting $\mathbf{E}$ instead of $\mathbf{C}$ is upper bounded at high SNRs by [5, 9]:

$$p(\mathbf{C} \rightarrow \mathbf{E}) \leq \frac{1}{2}\left(\frac{E_s}{4N_0}\right)^{-E_H \cdot N_r} (E_P)^{-N_r} , \quad (3)$$

where E_H is referred to as the *effective Hamming distance*, which quantifies the transmit diversity order and E_P is termed as the *effective product distance* [5], which quantifies the coding advantage of a space-time code.

It was shown in [10] that a full-transmitter-diversity STTC scheme having the minimum decoding complexity can be systematically designed based on two steps. The first step is to design a block code, while the second step is to transmit the block code diagonally across the space-time grid. The mechanism of the diagonal transmission across the space-time grid will be exemplified in Section 4 in the context of Figure 2. The Hamming distance and the product distance of a block code can be preserved, when the block code is transmitted diagonally across the space-time grid. Hence, a full-transmitter-diversity STTC scheme can be realised, when the Hamming distance of the block code used by the STTC scheme equals to the number of transmitters. Based on the same principle, a joint source coding and STTC scheme can be systematically designed by first designing a 2D VLC and then transmitting the 2D VLC diagonally across the space-time grid. As mentioned above [10], this allows us to achieve a transmitter-diversity order, which is identical to the Hamming distance of the 2D VLC plus a coding advantage quantified by the product distance of the 2D VLC, as well as a multiplexing gain, provided that the number of possible source symbols N_s is higher than the number of modulation levels M.

Let us now commence our detailed discourse on the proposed VL-STCM-ID scheme in the following sections.

3. TWO-DIMENSIONAL VLC DESIGN

Consider for example a source having $N_s = 8$ possible discrete values and let the lth value be represented by a symbol $s^l = l$ for $l \in \{1, 2, \ldots, N_s\}$. Furthermore, assume that the source is correlated such that the source symbol occurrence probability is given by:

$$P(s^{l+1}) = 0.6P(s^l) , \quad (4)$$

and $\sum_{l=1}^{N_s} P(s^l) = 1$. Hence, the source symbol s^1 has the highest occurrence probability of $P(s^1) = 0.406833$ and the source symbol s^8 has the lowest occurrence probability of $P(s^8) = 0.011389$. Let us now consider a 2D VLC codeword matrix, V_{VLC}, which encodes these $N_s = 8$ possible source symbols using $N_t = 3$ transmit antennas and BPSK modulation as follows:

$$\mathbf{V}_{VLC} = \begin{bmatrix} \text{x} & 1 & \text{x} & 0 & \text{x} & 0 & 1 & 1 \\ \text{x} & \text{x} & 0 & \text{x} & 1 & 1 & 0 & 1 \\ 0 & \text{x} & \text{x} & 1 & 1 & \text{x} & 1 & 0 \end{bmatrix} , \quad (5)$$

where each column of the (3×8)-dimensional matrix $\mathbf{V}_{VLC}$ corresponds to the specific VLC codeword conveying a particular source symbol and the elements in the matrix denoted as 0 and 1 represent the BPSK symbols to be transmitted by the $N_t = 3$ transmit antennas, while 'x' represents 'no transmission'. 'No transmission' implies that the corresponding transmit antenna sends no signal. Let the lth source symbol s^l be encoded using the mth column of the $\mathbf{V}_{VLC}$ matrix seen in Equation 5. Hence, the source symbol s^1 is encoded into an N_t-element codeword using the first column of $\mathbf{V}_{VLC}$ in Equation 5, namely [x x 0]^T, where the first and second transmit antennas are in the 'no transmission' mode, while the third antenna transmits an 'active' symbol represented by the binary value '0'. If $L(s^l)$ is the number of 'active' symbols in the VLC codeword assigned to source symbol s^l, then we may define the average codeword length of the 2D VLC as:

$$L_{ave} = \sum_{l=1}^{N_s} P(s^l) L(s^l) \ , \quad (6)$$

where we have $L_{ave} = 1.233$ bit/VLC codeword for this system according to Equations 4 and 5. The corresponding BPSK signal mapper is characterised in Figure 1, where the 'no transmission' symbol is actually represented by the origin of the Euclidean space, i.e. we have $f(\mathrm{x}) = 0$, where $f(.)$ is the mapping function. Since the 'no transmission' symbol is a zero energy symbol, the amount of energy saving can be computed from:

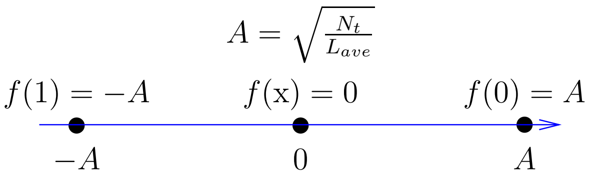

Figure 1: The signal mapper of the VL-STCM.

$$A^2 = \frac{N_t}{L_{ave}} \ , \quad (7)$$

where we have $A^2 = 3/1.233 = 2.433$, which is equivalent to $20\log(A) = 3.86$ dB. Hence, more transmitted energy is saved, when there are more 'no transmission' symbols in a VLC codeword. Therefore, the columns of the matrix $\mathbf{V}_{VLC}$ in Equation 5, which are the VLC codewords, and the source symbols are specifically arranged, so that the more frequently occurring source symbols are assigned to VLC codewords having more 'no transmission' components, in order to save transmit energy. The energy saved is then reallocated to the 'active' symbols for the sake of increasing their minimum Euclidean distance, as shown in Figure 1.

The design of the 2D VLC scheme can be summarised in the following three steps:

1. Search for all possible VLC codeword matrices, which have the maximum achievable minimum Hamming distance $E_{H\,\min}$ and product distance $E_{P\,\min}$ values for each pair of the VLC codewords at a given N_s and N_t combination. Note that attaining a higher $E_{H\,\min}$ is given more weight than $E_{P\,\min}$ since $E_{H\,\min}$, is more dominant in the PWEP of Equation 3.

2. From the resultant VLC matrices, choose that specific one, which has the highest number of 'no transmission' symbols at the given $E_{H\,\min}$ and $E_{P\,\min}$ combination.

3. Assign the more frequently occurring source symbols to the VLC codewords having more 'no transmission' components.

Additionally, we note that the correlation of the source only affects the specific mapping of the source symbols to the 2D VLC codewords, but not the search for the best 2D VLC itself, which takes place during steps 1 and 2. As in the conventional 1D VLC, the higher the source correlation, the lower the average codeword length L_{ave} of the 2D VLC. Hence, a higher power saving can be obtained, when the source is more correlated, since the amount of energy saving is given by Equation 7, where N_t is fixed. The 2D VLC matrix seen in Equation 5 was designed based on the above three steps and the corresponding minimum Euclidean distance of the BPSK constellation points seen in Figure 1 becomes identical to $A = 1.56$. The minimum Hamming distance is $E_{H\,\min} = 2$, as can be verified by counting the number of different symbol positions of all the columns in Equation 5. Hence a transmit-diversity of order $E_{H\,\min} = 2$ can be achieved instead of three, when $N_t = 3$ transmit antennas are employed for transmitting the N_t-element 2D VLC codewords denoted as $\mathbf{v} = [v_1 \ldots v_{N_t}]^T$ in Figure 2. On the other hand, the minimum product distance $E_{P\,\min}$ can be computed based on Equation 5 and the signal mapper of Figure 1. Explicitly, the corresponding minimum product distance is found to be $E_{P\,\min} = 5.92$, which is computed as [10]:

$$E_{P\,\min} \ = \ \min_{1 \le s < \tilde{s} \le N_s} \prod_{m \in \xi} |f(v_m) - f(\tilde{v}_m)|^2 \ , \quad (8)$$

where ξ is the specific VLC codeword component of Figure 2 mapped to transmit antenna index m associated with $v_m \neq \tilde{v}_m$ for $1 \le m \le N_t$, while $[v_1 \ldots v_{N_t}]^T$ and $[\tilde{v}_1 \ldots \tilde{v}_{N_t}]^T$ are two VLC codewords conveying the source symbols s and $\tilde{s}$, respectively.

4. VL-STCM TRANSMITTER

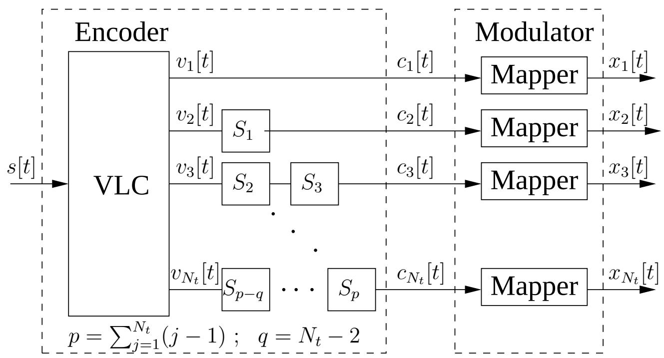

Figure 2: Block diagram of the VL-STCM transmitter.

The block diagram of the VL-STCM transmitter is illustrated in Figure 2. As seen in Figure 2, a VLC codeword $\mathbf{v}[t] = [v_1[t]\, v_2[t] \ldots\, v_{N_t}[t]]^T$ is assigned to each of the source symbols $s[t]$ generated by the source at time instant t, where $s[t] \in \{1, \ldots, N_s\}$ and N_s denotes the number of possible source symbols. Each component of the VLC codeword $\mathbf{v}[t]$ seen in Figure 2 is represented by a binary or non-binary symbol. Again, each of these VLC codewords corresponds to one

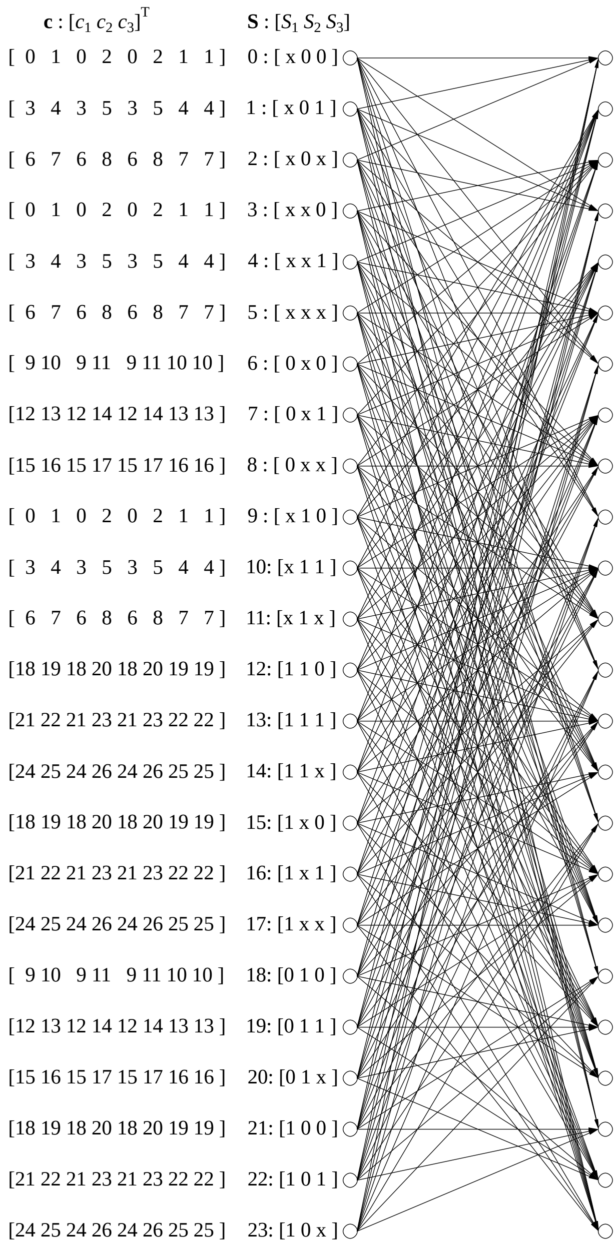

Figure 3: The trellis of VL-STCM when invoking the 2D VLC of Equation 5. For the list of codewords see Table 1.

of the columns in the VLC matrix of Equation 5. As portrayed in Figure 2, the VLC codeword $\mathbf{v}[t]$ is transmitted diagonally across the space-time grid with the aid of appropriate-length shift registers denoted as S_k in Figure 2, where we have $k \in \{1, 2, \ldots, \sum_{j=1}^{N_t}(j-1)\}$. As we can see from Figure 2, the codeword $\mathbf{v}[t] = [v_1[t]\ v_2[t]\ \ldots\ v_{N_t}[t]]^T$ is transmitted using N_t transmit antennas, where the mth element of each VLC codeword, for $1 \leq m \leq N_t$, is delayed by $(m-1)$ shift register cells, before it is transmitted through the mth transmit antenna. Hence, the N_t number of components of each VLC codeword are transmitted on a diagonal of the space-time codeword matrix of Equation 2. Since the VLC codewords are encoded diagonally, the space-time coded symbol $c_m[t]$ transmitted by the mth antenna, $1 \leq m \leq N_t$, at a particular time-instant t is given by $c_m[t] = v_m[t-m+1]$. Hence, for this specific case each element of the space-time codeword matrix of Equation 2 is given by $c_m[t] = v_m[t-m+1]$, while the transmitted signal is given by $x_m[t] = f(c_m[t]) = f(v_m[t-m+1])$ for $1 \leq m \leq N_t$.

Index	**c**	Index	**c**	Index	**c**
0	$[\,0\ \mathrm{x}\ \mathrm{x}\,]^T$	9	$[\,0\ 0\ \mathrm{x}\,]^T$	18	$[\,0\ 1\ \mathrm{x}\,]^T$
1	$[\,0\ \mathrm{x}\ 1\,]^T$	10	$[\,0\ 0\ 1\,]^T$	19	$[\,0\ 1\ 1\,]^T$
2	$[\,0\ \mathrm{x}\ 0\,]^T$	11	$[\,0\ 0\ 0\,]^T$	20	$[\,0\ 1\ 0\,]^T$
3	$[\,1\ \mathrm{x}\ \mathrm{x}\,]^T$	12	$[\,1\ 0\ \mathrm{x}\,]^T$	21	$[\,1\ 1\ \mathrm{x}\,]^T$
4	$[\,1\ \mathrm{x}\ 1\,]^T$	13	$[\,1\ 0\ 1\,]^T$	22	$[\,1\ 1\ 1\,]^T$
5	$[\,1\ \mathrm{x}\ 0\,]^T$	14	$[\,1\ 0\ 0\,]^T$	23	$[\,1\ 1\ 0\,]^T$
6	$[\,\mathrm{x}\ \mathrm{x}\ \mathrm{x}\,]^T$	15	$[\,\mathrm{x}\ 0\ \mathrm{x}\,]^T$	24	$[\,\mathrm{x}\ 1\ \mathrm{x}\,]^T$
7	$[\,\mathrm{x}\ \mathrm{x}\ 1\,]^T$	16	$[\,\mathrm{x}\ 0\ 1\,]^T$	25	$[\,\mathrm{x}\ 1\ 1\,]^T$
8	$[\,\mathrm{x}\ \mathrm{x}\ 0\,]^T$	17	$[\,\mathrm{x}\ 0\ 0\,]^T$	26	$[\,\mathrm{x}\ 1\ 0\,]^T$

Table 1: The space-time codeword table.

Note that originally there were only $N_s = 8$ legitimate 2D-VLC codewords in Equation 5. However, after these VLC codewords are diagonally mapped across the space-time grid using the shift registers shown in Figure 2, there is a total of $\bar{M}^{N_t} = 3^3 = 27$ legitimate space-time codewords, where $\bar{M}$ is the number of possible symbols in each position of the 2D VLC codewords. Note however that the actual number of legitimate space-time codewords can be less than $\bar{M}^{N_t}$. The corresponding trellis diagram of the proposed VL-STCM scheme is depicted in Figure 3. The $N_t = 3$-element space-time codeword seen in Figure 2 is given by $\mathbf{c} = [c_1\ c_2\ c_3]^T$ and the relationship between the 27 codeword indices shown in Figure 3 and $\mathbf{c}$ is defined in Table 1. The trellis states are defined by the contents of the shift register cells S_k shown in Figure 2, which are denoted by $\mathbf{S} = [S_1\ S_2\ S_3]$. For example, the state $\mathbf{S} = 0$ is denoted as [x 0 0] in the trellis diagram of Figure 3. Note that each shift register cell may hold $\bar{M} = 3$ possible values, namely $\{0, 1, \mathrm{x}\}$ in conjunction with the VL-STCM based on Equation 5. However, the number of legitimate trellis states can be less than $\bar{M}^p$, where $p = \sum_{j=1}^{N_t} = 3$ is the total number of shift registers. Hence, in our specific case there are only 24 legitimate trellis states out of the $\bar{M}^p = 27$ possible trellis states, which is a consequence of the constraints imposed by the 2D VLC of Equation 5.

5. VL-STCM-ID TRANSCEIVER

In order to invoke iterative detection and hence attain iteration gains as a benefit of the more meritoriously spread $extrinsic$ information, we introduce a symbol-based interleaver and a non-binary unity-rate precoder for each of the $N_t = 3$ transmit antennas. As we can see from Figure 4, each element in the space-time codeword $c_m[t]$ for $m \in \{1, 2, 3\}$ is further inter-

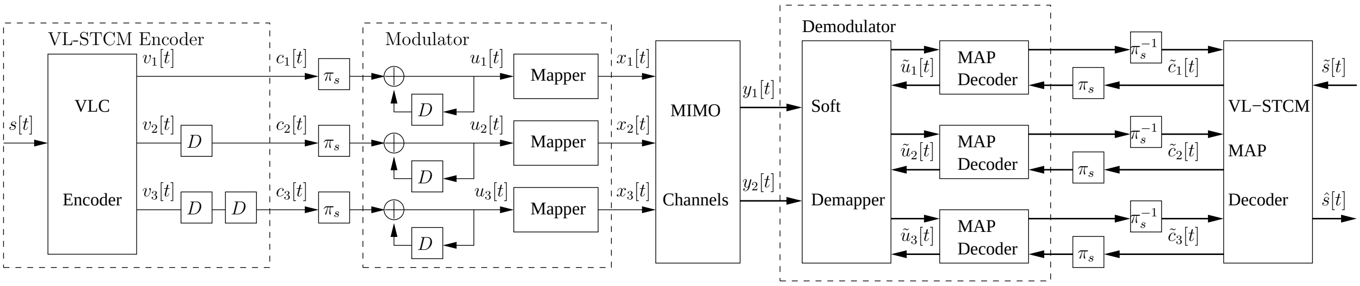

Figure 4: The VL-STCM-ID transceiver employing $N_t = 3$ transmit and $N_r = 2$ receive antennas. The notation $\tilde{(.)}$ and $\hat{(.)}$ indicates the $extrinsic$/$a\ priori$ probability and the hard decision estimate of $(.)$, respectively.

leaved and encoded by a non-binary unity-rate precoder, before feeding them to the mapper. It was found that without the recursive feedback assisted non-binary precoder, the iterative detection aided VL-STCM-ID was unable to outperform the lower-complexity non-iteratively decoded VL-STCM scheme. By contrast, a simple single-cell non-binary precoder invoked for each of the transmit antennas did allow us to achieve a significant iteration gain. The non-binary precoder employs a modulo-$\bar{M}$ adder, where again $\bar{M} = 3$ is the number of different symbols in the VLC space-time codeword and we have $c_m[t] \in \{0, 1, \mathrm{x}\}$. Accordingly, this single-cell precoder possesses $\bar{M} = 3$ trellis states.

At the receiver, the symbol-based MAP algorithm [11] is used by both the VL-STCM decoder and the unity-rate decoder. As we can see from Figure 4, the MAP decoder of the VL-STCM scheme benefits from the $a\ priori$ information of the space-time codeword $\mathbf{c}[t] = [c_1[t]\ c_2[t]\ c_3[t]]^T$ provided by the demodulator as well as from the $a\ priori$ information of the source symbols $s[t]$ quantified in terms of their different probabilities. Furthermore, each of the $N_t = 3$ unity-rate 'MAP Decoders' of the precoder seen inside the demodulator block of Figure 4 also benefits from the $a\ priori$ information of its codeword $u_m[t]$ and that of its input symbol $c_m[t]$, $m \in \{1, 2, \ldots, N_t\}$. The task of the soft demapper seen in the demodulator block of Figure 4 is to generate the soft metrics, characterising the probability of the transmitted space-time signal $x_m[t]$, $1 \leq m \leq N_t$, seen in Figure 1. The 'Soft Demapper' of Figure 4 also benefits from the $a\ priori$ information of its input symbols $u_m[t]$ after the first iteration, where a full iteration consists of a soft demapper operation, $N_t = 3$ unity-rate, MAP decoder operations and a VL-STCM MAP decoder operation. For the non-iteratively decoded VL-STCM, the soft demapper computes the $a\ priori$ information of $\mathbf{c}[t] = [c_1[t]\ c_2[t]\ c_3[t]]^T$ and feeds it to the VL-STCM MAP decoder.

6. SIMULATION RESULTS

Before we commence our performance study of the proposed scheme, we introduce a Fixed Length (FL) STCM (FL-STCM) benchmarker, where the FL Codeword (FLC) matrix is given by:

$$\mathbf{V}_{FLC} = \begin{bmatrix} 0 & 0 & 0 & 0 & 1 & 1 & 1 & 1 \\ 0 & 0 & 1 & 1 & 0 & 0 & 1 & 1 \\ 0 & 1 & 0 & 1 & 0 & 1 & 0 & 1 \end{bmatrix}. \quad (9)$$

The FL-STCM transmitter obeys the schematic of Figure 2, except that it employs the $\mathbf{V}_{FLC}$ of Equation 9. For the FL-STCM, the minimum Hamming distance and product distance are 1 and 4, respectively. It attains the same multiplexing gain as that of the VL-STCM or VL-STCM-ID arrangements. Let us now evaluate the performance of the VL-STCM, VL-STCM-ID and FL-STCM schemes in terms of their source Symbol Error Ratio (SER) versus the Signal to Noise Ratio (SNR) per bit, which is given by $E_b/N_0 = \gamma/\eta$, where γ is the SNR per receive antenna and $\eta = \log_2(8) = 3$ bit/symbol is the effective information throughput.

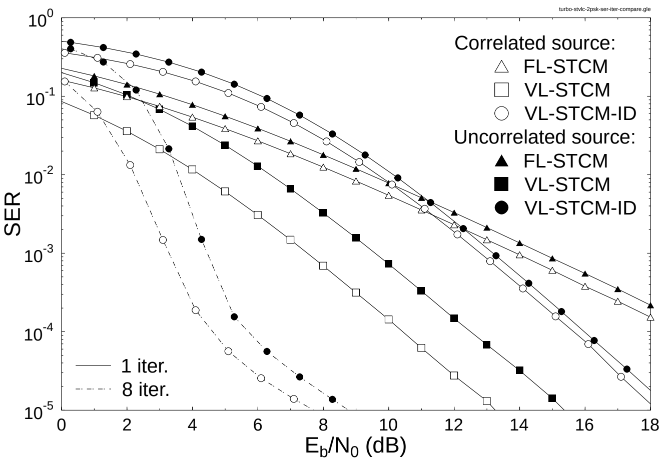

Figure 5: SER versus E_b/N_0 performance of the VL-STCM, VL-STCM-ID and FL-STCM schemes, when communicating over uncorrelated Rayleigh fading channels using BPSK, $N_t = 3$ and $N_r = 2$.

Figure 5 depicts the SER versus E_b/N_0 performance of the VL-STCM, VL-STCM-ID and FL-STCM schemes, when communicating over uncorrelated Rayleigh fading channels using BPSK, three transmitters and two receivers. As expected, the VL-STCM arrangement attains a higher gain, when the source has an adjacent-sample correlation of 0.6 compared to its uncorrelated counterpart. However, both the FL-STCM and VL-STCM-ID schemes still manage to achieve some coding gain, since their decoder benefits from the probability-related $a\ priori$ information of the source symbols. More specifically, the coding gain attained as a benefit of transmitting correlated source symbols increases, as the number of iterations invoked by the VL-STCM-ID scheme increases. Although the VL-STCM-ID arrangement performs worse than VL-STCM during the 1st iteration, the performance of VL-STCM-ID at SER$= 10^{-4}$ after the 8th iteration is approximately 5.7 (14.1) dB and 6.8 (14.3) dB better than that of the VL-STCM (FL-STCM) scheme, when employing correlated and uncorrelated sources, respectively.

7. CONCLUSIONS

An iteratively decoded variable length space-time coded modulation design was proposed. The joint design of source-coding, space-time coded modulation and iterative decoding was shown to achieve both spatial diversity and multiplexing gain, as well as coding and iteration gains at the same time. The variable length structure of the individual codewords mapped to the maximum of N_t transmit antennas imposes no synchronisation and error propagation problems. A significant iteration gain was achieved by the VL-STCM-ID scheme and it outperformed both the VL-STCM scheme as well as the FL-STCM benchmarker. Our future research will incorporate both explicit channel coding and real-time multimedia source codecs.

8. REFERENCES

[1] C. Shannon, *Mathematical Theory of Communication*. University of Illinois Press, 1963.

[2] G. Foschini Jr. and M. Gans, "On limits of wireless communication in a fading environment when using multiple antennas," *Wireless Personal Communications*, vol. 6, pp. 311–335, March 1998.

[3] E. Telatar, "Capacity of multi-antenna Gaussian channels," *European Transactions on Telecommunication*, vol. 10, pp. 585–595, Nov–Dec 1999.

[4] G. J. Foschini, Jr., "Layered space-time architecture for wireless communication in a fading environment when using multi-element antennas," *Bell Labs Technical Journal*, pp. 41–59, 1996.

[5] V. Tarokh, N. Seshadri and A. R. Calderbank, "Space-time codes for high rate wireless communication: Performance analysis and code construction," *IEEE Transactions on Information Theory*, vol. 44, pp. 744–765, March 1998.

[6] D. Divsalar, S. Dolinar and F. Pollara, "Serial concatenated trellis coded modulation with rate-1 inner code," in *GLOBECOM '00*, (San Francisco, CA), pp. 777–782, Nov–Dec 2000.

[7] G. Ungerböck, "Channel coding with multilevel/phase signals," *IEEE Transactions on Information Theory*, vol. 28, pp. 55–67, January 1982.

[8] A. F. Naguib, V. Tarokh, N. Seshadri and A. R. Calderbank, "A space-time coding modem for high-data-rate wireless communications," *IEEE Journal on Selected Areas in Communications*, vol. 16, pp. 1459 – 1478, October 1998.

[9] D. Divsalar and M.K. Simon, "Trellis coded modulation for 4800-9600 bits/s transmission over a fading mobile satellite channel," *IEEE Journal on Selected Areas in Communications*, vol. 5, pp. 162–175, February 1987.

[10] M. Tao and R. S. Cheng, "Diagonal block space-time code design for diversity and coding advantage over flat rayleigh fading channels," *IEEE Transactions on Signal Processing*, pp. 1012–1020, April 2004.

[11] L. Hanzo, T. H. Liew and B. L. Yeap, *Turbo Coding, Turbo Equalisation and Space Time Coding for Transmission over Wireless channels*. New York, USA: John Wiley IEEE Press, 2002.